Radiation Physics and Chemistry ∎ (∎∎∎∎) ∎∎∎–∎∎∎

Contents lists available at ScienceDirect

Radiation Physics and Chemistry

journal homepage: www.elsevier.com/locate/radphyschem

Effect of particle-size selectivity on quantitative X-ray dark-field computed tomography using a grating interferometer

Yuan Bao [a,b], Qigang Shao [a], Renfang Hu [a], Shengxiang Wang [a], Kun Gao [a], Yan Wang [b], Yangchao Tian [a,*], Peiping Zhu [a,b,**]

[a] National Synchrotron Radiation Laboratory, University of Science and Technology of China, Hefei 230026, China
[b] Institute of High Energy Physics, Chinese Academy of Science, Beijing 100049, China

HIGHLIGHTS

- Propose a method to differentiate materials of identical X-ray absorption.
- Quantitatively reconstruct the dark-field CT image with specific particle-size.
- Extend the application range of grating interferometer.

ARTICLE INFO

Article history:
Received 15 November 2015
Received in revised form
5 January 2016
Accepted 15 January 2016

Keywords:
Dark-field
Computed tomography
Grating interferometer
Particle-size

ABSTRACT

According to the conclusion of Khelashvili et al. [Phys. Med. Biol. 51, 221 (2006)], the minus logarithm of the visibility ratio fulfills the line integral condition; consequently the scattering information can be reconstructed quantitatively by conventional computed tomography (CT) algorithms. Based on Fresnel diffraction theory, we analyzed the influence of particle-size selectivity on the performance of an X-ray grating interferometer (GI) applied for dark-field CT. The results state the signal-to-noise ratio (SNR) of dark-field imaging is sensitive to the particle size, which demonstrate that the X-ray dark-field CT using a GI can efficiently differentiate materials of identical X-ray absorption and help to choose optimal X-ray energy for known particle size, thus extending the application range of grating interferometer.

1. Introduction

X-ray dark-field imaging, also referred to as (ultra) small angle X-ray scattering imaging, is a powerful tool for exploring the inaccessible spatially resolved information about the distribution of micron and submicron sized structural formations. While attenuation-based imaging needs higher X-ray radiation doses to improve contrast resolution for low attenuation matters, dark-field imaging does not intrinsically rely on photon absorption. Hence, X-ray energy in dark-field imaging can be optimized to minimize radiation damage to the sample. An X-ray grating-based dark-field imaging was proposed by Pfeiffer et al. (Lynch et al., 2011; Pfeiffer et al., 2008; Wang et al., 2009; Wen et al., 2009) which can produce high-quality X-ray dark-field images using X-ray tube source based on the visibility degradation of the oscillation curves. Now, X-ray dark-field imaging has drawn an increasing attention and become a research highlight in biomedical and materials science imaging (Bao et al., 2015; Chabior et al., 2011; Cong et al., 2012; Doronina-Amitonova et al., 2013; Endrizzi et al., 2014; Grunzweig et al., 2013; Jensen et al., 2010; Lee et al., 2013).

Computed tomography (CT) requires the reconstructed signal fulfills the line integral condition. In diffraction enhanced imaging, Khelashvili et al. (2006) and Yashiro et al. (2010) assumed the ultra-small angle X-ray scattering parameter is also a line integral of object thickness as well as the absorption and refraction parameters. Wang et al. (2009) deduced the relationship between the second moment of scattering angle distribution and the visibility degradation of the oscillation curve with Fourier transform method and established the quantitative theoretical framework of dark-field CT for the grating-based method. Lynch et al. (2011) showed that the fringe visibility decays exponentially with the sample thickness when the fringes are geometric projections of Ronchi-type gratings and that the DFEC (dark-field extinction coefficient) is determined by an auto-correlation of the electron density distribution.

The present work on extracting dark-field information is mainly motivated by the fact that the scattering coefficient is

* Corresponding author.
** Corresponding author at: National Synchrotron Radiation Laboratory, University of Science and Technology of China, Hefei 230026, China.
E-mail addresses: ychtian@ustc.edu.cn (Y. Tian), zhupp@ihep.ac.cn (P. Zhu).

http://dx.doi.org/10.1016/j.radphyschem.2016.01.022
0969-806X/

related to X-ray energy and particle size. However, the analysis about their influence are lacking for dark-field CT. Through wave-optical numerical simulations, we show the SNR of dark-field imaging is sensitive to special particle size. The present analysis can also be extended to Talbot-Lau geometry (Engelhardt et al., 2008; Momose et al., 2006; Pfeiffer et al., 2006, 2007; Weitkamp et al., 2005, 2006.) and to the scanning double-grating configuration (Nesterets and Wilkins, 2008).

2. Methods

X-ray refraction and diffraction both arise from spatial variations of the refractive index in the sample material, but on different length scales. X-ray refraction is caused by macroscopic variations of the refractive index in the sample that are resolved by the imaging detector. Diffraction, or coherent scattering, is caused by unresolved, microscopic fluctuations of the refractive index. In coherent scattering, both the cross section and the angular distribution are dependent on the length scale of the scattering structures, so the dark-field extinction can potentially be used to characterize materials containing micro-scattering structures.

In the grating-based imaging system (Fig. 1), an absorption or phase grating (G1) is used to split the incident X rays to create a periodic intensity pattern, i.e., Talbot self-imaging effect. Another absorption grating (G2) positioned at the plane of the self-image acts an analyzer. A scattering object placed in the incident parallel beam will cause slight refraction within a pixel and therefore modifications of the original wave-front. The scattered X rays can be described by a scattering angle distribution which can be assumed to follow the Gaussian distribution. The second moment of the scattering angle distribution measures the broadening of the rays, which is

$$\sigma^2 = \int \Delta\theta_s^2 p(\Delta\theta_s) d\Delta\theta_s \tag{1}$$

where $\Delta\theta_s$ is the scattering angle, relative to the incident direction of X rays and $p(\Delta\theta_s)$ is the scattering angle distribution which is

$$p(\Delta\theta_s) = \frac{1}{\sigma\sqrt{2\pi}} \exp\left[-\frac{(\Delta\theta_s)^2}{2\sigma^2}\right] \tag{2}$$

Wang et al. (2009) has established a quantitative relationship between the second moment of the scattering angle distribution and the visibility degeneration of the oscillation curve

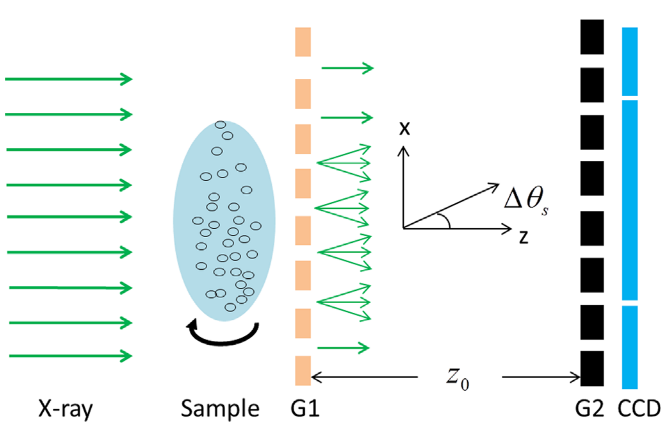

Fig. 1. The diagram of X-ray dark-field computed tomography using a grating interferometer.

$$\sigma^2 = -\frac{1}{2\pi^2}\left(\frac{d}{z_0}\right)^2 \ln\left(\frac{V'}{V}\right) \tag{3}$$

Also, Yashiro et al. (2010) arrived at a similar conclusion which is

$$-\ln\left[\frac{V}{V_0}\right] \approx \int \frac{\partial\left(\sigma^2(z)\right)}{\partial z}[1-\gamma(z)]dz \tag{4}$$

where σ and γ are expressed as functions of z, $\partial(\sigma^2(z))/\partial z$ is proportional to the square of the X-ray wavelength λ^2 and the square of the number density of electrons $(\Delta\rho)^2$. Thus, we can also carry out tomography and determine the three-dimensional distribution of $(1-\gamma)\partial(\sigma^2)/\partial z$.

Moreover, Khelashvili et al. (2006) has deduced that the second moment of the scattering angle distribution fulfills the line integral condition, which is

$$\sigma^2 = \int_0^L S(l)\, d\, l = \int_0^L \left[\frac{\rho_n(l)\sigma_s(l)}{2\alpha_p}\right] d\, l \tag{5}$$

where S represents the generalized scattering parameter of the X-ray, ρ_n is the density of the sample, σ_s is the scattering cross section and α_p represents angular beam broadening due to a single spherical scatter and relates to the incident X ray energy, which are expressed as follows, respectively

$$\sigma_s = \pi r^2 \tag{6}$$

$$\alpha_p = \frac{1}{4(\delta(\lambda))^2 \ln\left(\frac{2}{\delta(\lambda)}+1\right)} \tag{7}$$

where r is the mean radius of the scattering microspheres, $\delta(\lambda)$ is the refractive index decrement.

Therefore, one can establish the quantitative relations between the scattering angle distribution and particle size, then quantitatively reconstruct scattering coefficient with conventional CT algorithms.

In addition, the measurement of signal-to-noise ratio (SNR) provides a useful indicator of gross imaging performance. SNR is defined as the ratio of the difference between the reconstructed scattering coefficient of the ROI within an object and its background to the detected noise. The detected noise is the square root of the mean of the squared standard deviations calculated in the two areas (Baldelli et al., 2009)

$$SNR = \frac{I_{ROI} - I_{BACK}}{\sqrt{\frac{\sigma_{ROI}^2 + \sigma_{BACK}^2}{2}}} \tag{8}$$

where I_{ROI} is the mean scattering coefficient in the ROI, I_{BACK} is the mean scattering coefficient in the nearby background, σ_{ROI} and σ_{BACK} are the standard deviations of the scattering coefficient in the ROI and in the nearby background, respectively. This study describes the SNR of the dark-field imaging with the varied designed energies or particle-size.

3. Simulations

In the computer simulation experiment, the simulated sample was Shepp-Logon phantom (Wang et al., 2009), the pixel values were the second moment of scattering angle distribution of PMMA micro particles instead of the attenuation coefficient. The sample was rotated with 1° increments within 180°. A phase-stepping process was implemented to produce the two intensity oscillation